Evaluation of thermal resistance constitution for packaged AlGaN/GaN high electron mobility transistors by structure function method*

Zhang Guang-Chen(张光沉)†, Feng Shi-Wei(冯士维), Zhou Zhou(周 舟), Li Jing-Wan(李静婉), and Guo Chun-Sheng(郭春生)

School of Electronic Information and Control Engineering, Beijing University of Technology, Beijing 100124*, China*

(Received 6 September 2010; revised manuscript received 20 September 2010)

The evaluation of thermal resistance constitution for packaged AlGaN/GaN high electron mobility transistor (HEMT) by structure function method is proposed in this paper. The evaluation is based on the transient heating measurement of the AlGaN/GaN HEMT by pulsed electrical temperature sensitive parameter method. The extracted chip-level and package-level thermal resistances of the packaged multi-finger AlGaN/GaN HEMT with 400-μm SiC substrate are 22.5 K/W and 7.2 K/W respectively, which provides a non-invasive method to evaluate the chip-level thermal resistance of packaged AlGaN/GaN HEMTs. It is also experimentally proved that the extraction of the chip-level thermal resistance by this proposed method is not influenced by package form of the tested device and temperature boundary condition of measurement stage.

Keywords: high electron mobility transistor, self-heating effect, structure function, reliability

PACS: 72.80.Ey, 73.40.Ns **DOI:** 10.1088/1674-1056/20/2/027202

1. Introduction

Attracting wide research interests over the past decade,[1−3] AlGaN/GaN based high electron mobility transistors (HEMTs) present unparalleled power and microwave performance at high drain-source voltage bias, such as continuous-wave power density 41.4 W/mm (on SiC substrate)[4] and 5.1 W/mm at 18 GHz (on Si substrate).[5] Consequently, special attention should be paid to the thermal management when devices and circuits are designed and modeled.[6] High channel temperature rise induced by the thermal dissipation of input power will lead to current collapse at high drain-source voltage, known as the self-heating effect, which significantly affects the device performance and long term reliability.[7] Therefore, accurate evaluation of the channel temperature and channel-to-case thermal resistance constitution is a prior task for designer of AlGaN/GaN HEMTs.

The main challenge of the channel temperature measurement for AlGaN/GaN HEMTs is the ultra-small area of channel region (usually less than 3 μm of the gate-drain gap), which makes the infrared image method out of the candidates.[8] One of the well-recognized solutions is the micro-Raman spectroscopy reported by Kuball *et al.*,[9] which achieves a temperature resolution of 10 °C and space resolution of 1 μm. Electrical temperature sensitive parameter (TSP) method is another popular choice. Menozzi *et al.*[10] overviewed the method of channel temperature prediction by DC I–V curves, which is very simple and non-invasive. However, the drawback of the micro-Raman method is the crucial demand of wave-number resolution of Raman spectroscopy and nanometer-level of stage controlling fixture. The disadvantage of the DC I–V method is the need of relying on dramatic assumption, such as the assumption that the thermal resistance is independent of temperature and dissipated power, which will induce intrinsic measurement error due to the existence of the temperature non-linearity of thermal conductivity and other temperature sensitive parameters. Furthermore, both of the methods cannot provide thermal resistance constitution analysis. In order to evaluate the chip level thermal resistance, the chip is always demanded to be directly mounted to an infinite heat sink to eliminate the package-level thermal resistance, which seriously restricts the usage of these methods.

*Project supported by the Natural Science Foundation of Beijing, China (Grant No. 4092005), the National High Technology Research and Development Program of China (Grant No. 2009AA032704), and the Specialized Research Fund for the Doctoral Program of Higher Education of China (Grant No. 20091103110006).

†Corresponding author. E-mail: zhangguangchen98@hotmail.com

© 2010 Chinese Physical Society and IOP Publishing Ltd

The structure function method based on the transient heating response measurement has been proved to be suitable for evaluating the thermal resistance constitution on the heat flow path, which was first proposed by Szekly[11] and has been successfully applied to thermal analysis of ICs[12,13] and LEDs.[14,15] However, because HEMTs are normally operated at negative gate-source voltage, which is not compatible with commercial thermal resistance tester needing positive TSP, such as T3ster[16] etc., the transient heating response curve measurement of AlGaN/GaN HEMT and related thermal resistance constitution evaluation has not been published, to the best of our knowledge. In the present paper, for the first time, we present the thermal resistance constitution evaluation of packaged AlGaN/GaN HEMTs by structure function method, which is based on the measurement of transient heating response curve by pulsed-switch electrical TSP method. By this method, the chip-level thermal resistance can be extracted from the channel-to-case thermal resistance and be analysed without the influence on package form and temperature boundary conditions of measurement stage.

2. Theoretical background

The structure function evaluation is based on the measurement of transient heating response curve of a specific heat flow system excited by a power step-excitation. The detailed algorithm can be found in Ref. [17] proposed by Szekly. Herein the procedure will be briefly outlined. Figure 1 shows a typical flow-chart of the structure function evaluation for a heat flow system with three main thermal resistance components.

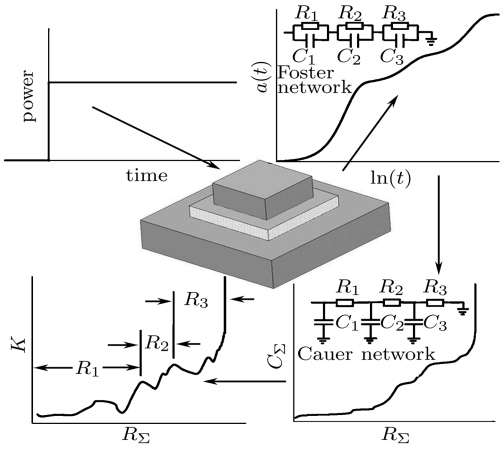


Fig. 1. Flow-chart of a typical structure function evaluation for a heat flow system with three main thermal resistance components.

The heat flow system consists of a series of components with different materials and geometrical sizes, such as chip, solder joint, package body for semiconductor devices. When an excitation power is applied to the active region of the device, the temperature rise of the active region with respect to the power applying time, so-called transient heating response curve (heating curve), can be considered as the response of a Foster thermal resistance and capacitance (RC) network model as shown in Fig. 1. The response can be characterized as follows:

$$a(t) = P \times \sum_{i=1}^{n} R_i(1 - \mathrm{e}^{-t/\tau_i}), \qquad (1)$$

where $a(t)$ is the heating curve, P is the excitation power, R_i is the thermal resistance of the i-th stage of the Foster RC network, $\tau_i = R_i \times C_i$ is the time constant of the i-th stage, t is the power applying time. Then, the values of R_i and C_i can be extracted from the time-constant spectrum by numerical deconvolution of the heating curve.[18] Because the node-to-node thermal capacitance in Foster network does not have obvious physical meaning, it is necessary to transform the Foster network to Cauer network as shown in Fig. 1, which has node-to-ground thermal capacitance to characterize the real heat flow structure. The transformation can be achieved by the impedance conservation method in the network synthesis theory.[19] With this network, the sum of thermal capacitance (C_Σ) with respect to the sum of thermal resistance (R_Σ), so-called cumulative structure function curve, can be drawn. By differentiating C_Σ with respect to R_Σ, the differential structure function curve can also be plotted. $\mathrm{d}C_\Sigma/\mathrm{d}R_\Sigma$ is named as K, and it could be expressed as

$$K(R_\Sigma) = \mathrm{d}C_\Sigma/\mathrm{d}R_\Sigma = \frac{cA\mathrm{d}x}{\mathrm{d}x/\lambda A} = c\lambda A^2, \qquad (2)$$

where c is the volumetric heat capacitance, λ is the thermal conductivity, and A is the cross-sectional area of the heat flow. For a specific layer in the heat flow path, the values of c and λ are both constant and A value increases in the heat conduction process because of the heat spreading effect. Therefore, the local peaks observed in the differential structure function indicate the reaching of new surface/material in the heat flow path as the result of abrupt variations of c and λ, and the thermal resistance of this partial component can be read from the distance on the horizontal

axis as shown in Fig. 1. Therefore, the thermal resistance constitution of AlGaN/GaN HEMTs can also be obtained by structure function evaluation with the measurement of the heating response curve. In the next section, we will describe the experiment apparatus and measurement process of the transient heating response curve of AlGaN/GaN HEMT.

3. Experimental apparatus and method

The AlGaN/GaN HEMT consisting of 25-nm un-intentional doped AlGaN on 1.5-μm GaN buffer layer on a 400-μm thick 4H–SiC substrate, with Ti/Al/Ni/Au drain, source Ohmic contacts and Ni/Au Schottky contact are investigated in this paper. The device is composed of 10 fingers each with a gate length of 0.35 μm, gate width of 100 μm, source-drain gap of 4.5 μm and gate-source gap of 1.5 μm. The gate and source contacts are formed by the air-bridge structure. Devices are passivated by a SiN layer of 100 nm. The device structure of the AlGaN/GaN HEMT and the micrograph of the chip are shown in Fig. 2. The chip is soldered on a cupric case with dimensions of 3 mm$\times$ 10 mm$\times$ 1 mm.

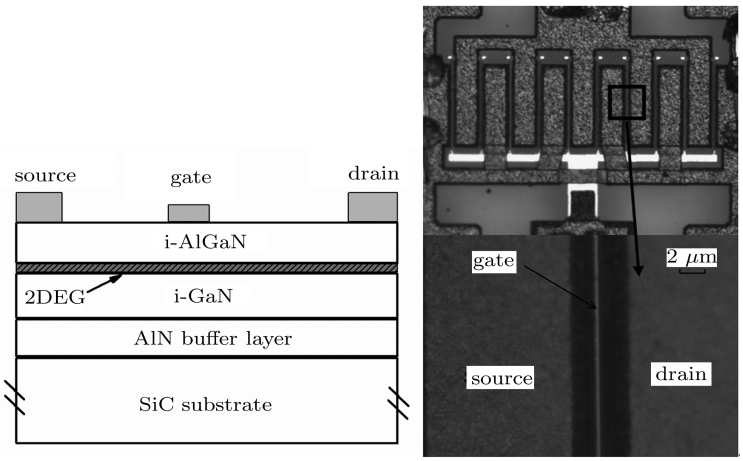


Fig. 2. Schematic (a) and micro-image (b) of the tested AlGaN/GaN HEMTs.

The forward voltage of the gate-source Schottky junction ($V_{\rm GSf}$) is selected to be the TSP in this work. Figure 3(a) shows the temperature dependence of $V_{\rm GSf}$, so-called calibration curve, tested in a DESPATCH temperature oven with a temperature accuracy of $\pm$1 °C. The drain terminal of the device under test (DUT) is left open and forward testing currents are chosen to be 0.5, 1.0, 1.5 and 2.0 mA respectively, which are low enough to avoid the self-heating effect, and then the $V_{\rm GSf}$ is recorded at different oven temperatures varying from 30 °C to 90 °C. The calibration curves present good linearity in the tested temperature range and the temperature coefficients (α) are –1.95, –1.80, –1.72, and –1.65 mV/K derived respectively from slopes of the calibration curves in Fig. 3(a). After the calibration of the temperature coefficient of $V_{\rm GSf}$, the channel temperature can be obtained by pulsed switching technique. Noting that gate-source voltage ($V_{\rm GS}$) is negatively biased and the drain-source voltage ($V_{\rm DS}$) is applied in the operation state, while the TSP is valid in the forward biased state, it is necessary to turn off $V_{\rm DS}$ firstly, then to forward bias the gate-source Schottky junction and to sample the shifting of TSP. The sequence diagram is shown in Fig. 3(b), where $t_{\rm h}$ is the heating time, $t_{\rm c}$ is the cooling time, and $t_{\rm d}$ is the delay time of the transition. The testing accuracy is seriously affected by the delay time and $t_{\rm d}$ of about 1 μs is achieved in our measurement.

The DUT is set on a constant temperature plate (40 °C in this experiment). A 2-mA test current is chosen and α is –1.65 mV/K. $I_{\rm DS}$ is set to about 100 mA and $V_{\rm DS}$ is 10 V. The first effective point of $\Delta V_{\rm GSf}$ is sampled in 1 μs, then 50 points of $V_{\rm GSf}(t)$ are recorded at 1-MHz sampling rate. The cooling curve is obtained by the measured shifting of $V_{\rm GSf}$ and the temperature coefficient as shown in Fig. 4(a). The tested cooling curve is fitted exponentially and the channel temperature rise at specific $t_{\rm h}$ ($a(t_{\rm h})$) is obtained by regress calculation.

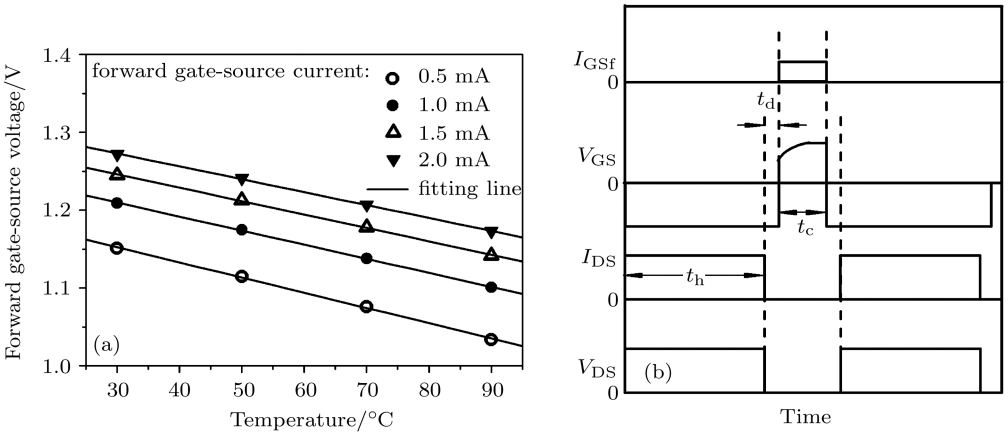


Fig. 3. (a) Calibration curve of the forward gate-source voltage, and (b) sequence diagram of the testing system.

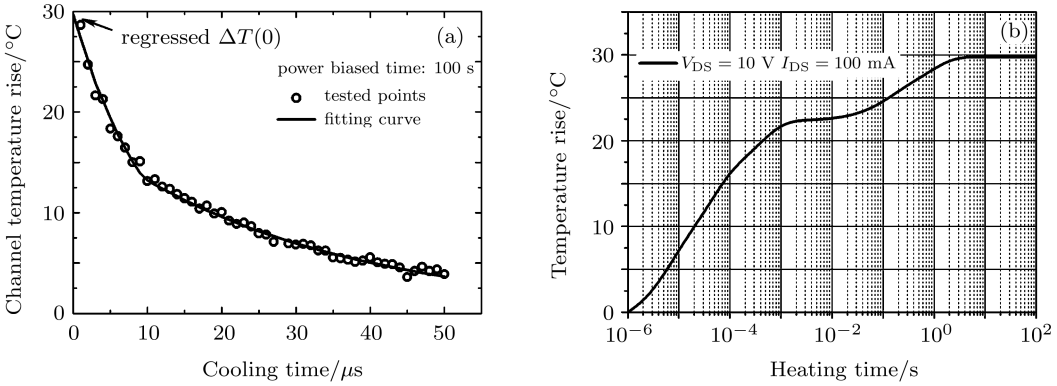


Fig. 4. (a) Cooling curve of the channel temperature rise, and (b) tested transient heating response curve at 10 V of V_{DS} and 100 mA of I_{DS}.

The transient heating response curves of AlGaN/GaN HEMTs can be recorded by maintaining the same initial temperature condition and multi-time heating operation with the increasing step of heating time in natural logarithm axis. There exists a trade-off between the accuracy and the testing time based on the selection of time step resolution. We find that a time resolution of about 0.2 on the logarithm time axis is an acceptable optimization. The tested heating curve of channel temperature rise is shown in Fig. 4(b) in the biased condition of 100 mA of I_{DS} and 10 V of V_{DS}. Hereby, with the measured heating curve, the corresponding structure function evaluation can be performed and will be presented in the next section.

4. Results and discussion

According to the procedure introduced in Section 1, the cumulative structure function curve can be obtained by plotting the cumulative thermal capacitance of the Cauer network with respect to the corresponding cumulative thermal resistance. More intuitive result of the thermal resistance constitution can be observed in the differential structure function curve by the differentiation of the cumulative structure function curve. The cumulative structure function and the differential structure function calculated based on Fig. 4(b) are shown in Fig. 5.

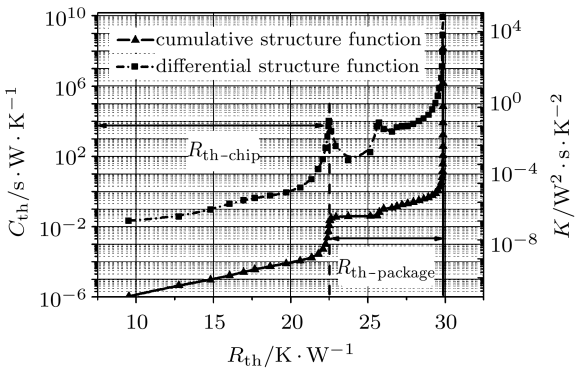


Fig. 5. Cumulative structure function and differential structure function, with I_{DS} being 100 mA, V_{DS} 10 V, and the temperature of constant temperature stage 40 °C.

The first strong and clear peak occurs at about 22.5 K/W of thermal resistance in the differential curve. According to the heat flow path of the tested sample, this peak should represent the thermal resistance of the first component in the channel-to-case thermal resistance, the chip-level thermal resistance. The thermal capacitance in the cumulative curve presents an abrupt increase at 22.5 K/W of thermal resistance, and then increases smoothly until the steady-state thermal resistance of 29.7 K/W, which indicates that the 7.2 K/W of thermal resistance, from 22.5 K/W to 29.7 K/W, is induced from the package body, because of the relatively large thermal capacitance of the cupric case. In order to confirm this conclusion, we have also measured the heating curves of the tested sample in air convection condition and in the condition with a cupric sheet between the case and the constant temperature stage separately. Both of the measurements intent to modify the package-level thermal resistance and have no influence on the chip-level thermal resistance. The biased condition is 100 mA of $I_{\rm DS}$ and 10 V of $V_{\rm DS}$ too, and the corresponding differential structure function curves are shown in Fig. 6.

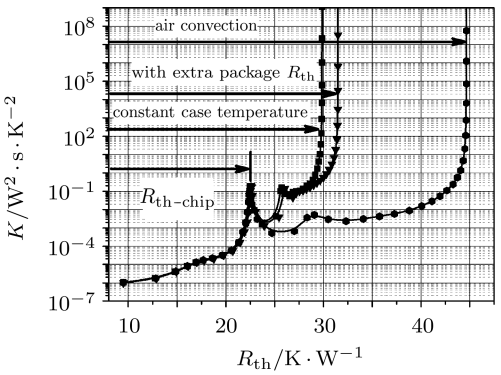


Fig. 6. Differential structure function of the tested device; the curve with square symbols represents the measurement at constant case temperature; the curve with triangle symbols represents the measurement with a cupric sheet between the case and the constant temperature stage; the curve with the circle symbols represents the measurement in boundary condition of air convection.

It is observed that the first peaks in Fig. 6 keep constant, while the steady-state thermal resistance in air convection condition (channel-to-atmospheric thermal resistance) reaches 44 K/W, which is because the case temperature keeps rising without the constant temperature stage until the thermal equilibrium with the air temperature is built. The curve with cupric sheet deviates from that with constant case temperature at about 28 K/W of thermal resistance, and the corresponding steady-state thermal resistance reaches 31.5 K/W. The separation between the two curves is the induced thermal resistance by the cupric sheet. The experimental results are consistent with those from the transient heating conduction theory. It is also verified that the first peak does represent the chip-level thermal resistance and is not influenced by the package form and temperature boundary condition in the process of structure function evaluation. Therefore, the chip-level thermal resistance is extracted from the channel-to-case thermal resistance by the transient heating measurement and structure function evaluation, which provides an accurate and convenient solution for the thermal management and optimization of AlGaN/GaN HEMTs.

5. Conclusion

The thermal resistance constitution evaluation of packaged AlGaN/GaN HEMTs is proposed by structure function method for the first time. The evaluation is based on the transient heating response curve measurement of the DUT by pulsed electrical method with selecting the forward gate-source Schottky voltage as TSP. The 22.5 K/W of chip-level thermal resistance of the tested packaged AlGaN/GaN HEMT sample is extracted from the 29.7 K/W of the channel-to-case thermal resistance, which provides a convenient method to evaluate the chip-level thermal characterization of packaged AlGaN/GaN HEMTs without strict requirement of constant temperature condition.

Acknowledgment

We express special thanks to Mr. Chen Tang-Sheng, Nanjing Electronic Devices Institute, for his valuable suggestions.

References

[1] Fan L, Hao Y, Zhao Y F, Zhang J C, Gao Z Y and Li P X 2009 *Chin. Phys.* B **18** 2912

[2] Gu W P, Duan H T, Ni J Y, Hao Y, Zhang J C, Feng Q and Ma X H 2009 *Chin. Phys.* B **18** 1601

[3] Ren F, Hao Z B, Wang L, Wang L, Li H T and Luo Y

2010 *Chin. Phys.* B **19** 017306

[4] Wu Y F, Moore M, Saxler A, Wisleder T and Parikh P 2006 *Device Research Conference* **64** 151

[5] Ducatteau D, Minko A, Hoël V, Morvan E, Delos E, Grimbert B, Lahreche H, Bove P, Gaquière C, De Jaeger J C and Delage S 2006 *IEEE Electron Device Lett.* **27** 7

[6] Chattopadhyay M K and Tokekar S 2008 *Microelectron. J.* **39** 1181

[7] Alamo J A and Joh J 2009 *Microelectron Reliab.* **49** 1200

[8] Darwish A M, Bayba A J and Hung H A 2008 *IEEE Trans. Microwave Theory Tech.* **56** 3188

[9] Kuball M, Hayes J M, Uren M J, Martin T, Birbeck J C H, Balmer R S and Hughes B T 2002 *IEEE Electron Device Lett.* **25** 7

[10] Menozzi R, Umana-Membreno G A, Nener B D, Parish G, Sozzi G, Faraone L and Mishra U K 2008 *IEEE Trans. Device Mater. Res.* **8** 255

[11] Szekely V 1997 *Microelectron. J.* **28** 277

[12] Rencz M 2005 *IEEE SEMI-THERM Symposium* **21** 307

[13] Poppe A, Zhang Y, Wilson J, Farkas G, Szabó P, Parry J, Rencz M and Székely V 2009 *IEEE Trans. Compon. Pack. T.* **32** 484

[14] Hu J Z, Yang L Q, Hwang W J and Shin M W 2006 *J. Crystal Growth* **288** 157

[15] Kim L, Choi J H, Jang S H and Shin M W 2007 *Thermochim. Acta* **455** 21

[16] Yang L Q, Hu J Z, Kim L and Shin M W 2008 *IEEE Trans. Device Mater. Res.* **8** 571

[17] Szekely V 2002 *Microelectron Reliab.* **42** 629

[18] Kennett T J, Prestwich W V and Robertson A 1978 *Nuclear Instruments and Methods* **151** 285

[19] Weinberg L 1962 *Network Analysis and Synthesis* (New York: McGraw-Hill) p. 366